Vitamin D_3 Metabolism in Human Glioblastoma Multiforme: Functionality of CYP27B1 Splice Variants, Metabolism of Calcidiol, and Effect of Calcitriol

Britta Diesel,[1] Jens Radermacher,[1] Matthias Bureik,[2] Rita Bernhardt,[2] Markus Seifert,[3] Jörg Reichrath,[3] Ulrike Fischer,[1] and Eckart Meese[1]

Abstract

Purpose: A better understanding of the vitamin D_3 metabolism is required to evaluate its potential therapeutic value for cancers. Here, we set out to contribute to the understanding of vitamin D_3 metabolism in glioblastoma multiforme.

Experimental Design: We did nested touchdown reverse transcription-PCR (RT-PCR) to identify CYP27B1 splice variants and real-time RT-PCR to quantify the expression of CYP27B1. A cell line was treated with calcitriol to determine the effect on the expression of CYP27B1, 1α,25-dihydroxyvitamin D_3-24-hydroxylase (CYP24), and vitamin D_3 receptor (VDR). We generated three antibodies for the specific detection of CYP27B1 and splice variants. High-performance TLC was done to determine the endogenous CYP27B1 activity and the functionality of CYP27B1 splice variants. Using WST-1 assay, we determined the effect of vitamin D_3 metabolites on proliferation.

Results: We report a total of 16 splice variants of CYP27B1 in glioblastoma multiforme and a different expression of CYP27B1 and variants between glioblastoma multiforme and normal tissues. We found preliminary evidence for enzymatic activity of endogenous CYP27B1 in glioblastoma multiforme cell cultures but not for the functionality of the splice variants. By adding calcitriol, we found a proliferative effect for some cell lines depending on the dose of calcitriol. The administration of calcitriol led to an elevated expression of CYP27B1 and CYP24 but left the expression of the VDR unaltered.

Conclusions: Our findings show that glioblastoma multiforme cell lines metabolize calcidiol. In addition, we show various effects mediated by calcitriol. We found a special vitamin D_3 metabolism and mode of action in glioblastoma multiforme that has to be taken into account in future vitamin D_3–related therapies.

The classic metabolism of the secosteroid hormone vitamin D_3 to its active form followed by several degradation pathways is well described. Vitamin D_3 is hydroxylated in the liver to 25-hydroxyvitamin D_3 [25-(OH)D_3 or calcidiol]. The further hydroxylation to the most active metabolite of vitamin D_3, 1α,25-dihydroxyvitamin D_3 [1α,25-$(OH)_2D_3$ or calcitriol], is mediated by CYP27B1 in the kidney. 24-Hydroxylation by 1α,25-dihydroxyvitamin D_3-24-hydroxylase (CYP24) is the first step of the main inactivating pathway, resulting in metabolites with decreased activity. The effects of calcitriol on target cells are mediated via binding to the nuclear vitamin D receptor (VDR) that functions as a ligand-dependent transcription factor (1). However, there is increasing evidence for the involvement of nongenomic pathways, mediated by a proposed membrane receptor (2, 3).

Besides renal CYP27B1 activity, extrarenal CYP27B1 expression has been described in a variety of tissues (4). *In vitro*, several nonrenal cells, including microglial cells (5), produce calcitriol from its precursor. In addition, several cancer cells show CYP27B1 activity (e.g., human non–small cell lung carcinoma cells; ref. 6). Local production of calcitriol has been postulated to play an autocrine or paracrine role in vitamin D–mediated growth control (7).

As shown for numerous normal and cancer cell lines, calcitriol is at high concentrations (10^{-9} to 10^{-6} mol/L) an antiproliferative and prodifferentiating agent that induces apoptosis and inhibits cell migration (8). The antiproliferative properties of calcitriol, as described above, were also shown for central nervous system tumors, including glioblastoma cell lines (9). Beneficial effects of the vitamin D_3 metabolite 1α-hydroxyvitamin D_3 have been reported for the treatment of glioblastoma multiforme in a small phase II clinical study (10). Its properties in regulating cancer cell growth make the

Authors' Affiliations: [1]Institut für Humangenetik, Theoretische Medizin; [2]Biochemie, Universität des Saarlandes, Saarbrücken, Germany; and [3]Hautklinik und Poliklinik der Universitätskliniken des Saarlandes, Homburg/Saar, Germany
Received 9/24/04; revised 3/31/05; accepted 4/6/05.

Grant support: Deutsche Forschungsgemeinschaft grant Fi644/1-1.

The costs of publication of this article were defrayed in part by the payment of page charges. This article must therefore be hereby marked *advertisement* in accordance with 18 U.S.C. Section 1734 solely to indicate this fact.

Note: Supplementary data for this article are available at Clinical Cancer Research Online (http://clincancerres.aacrjournals.org/).

U. Fischer and E. Meese share equal contribution as senior authors.

Requests for reprints: Eckart Meese, Institut für Humangenetik, Universitätskliniken des Saarlandes, Geb. 60, 66421 Homburg/Saar, Germany. Phone: 49-6841-162-6038; Fax: 49-6841-162-6186; E-mail: hgemee@uniklinikum-saarland.de.

hormone of potential interest in the management of tumors and lead to the development of a broad variety of analogues with weaker calcemic side effects (11).

Previously, we reported gene amplification and mRNA splice variants of the gene encoding the *P*450 cytochrome 25-hydroxyvitamin D_3-1α-hydroxylase in human glioblastoma multiforme (12).

Gene amplifications are frequent in glioblastoma multiforme, including an amplicon at chromosome 12q13-15 that contains the gene for CYP27B1. The relatively high amplification frequency (16%) of the *CYP27B1* gene (12)[4] suggests that this gene may be, beside others, a likely target gene of the amplification unit 12q13-15.

As already described for other cytochrome *P*450 genes (13), alternative splicing can play a role in regulating the enzyme level and may cause tissue-specific variations in healthy cells. A number of studies show that alternative splicing occurs frequently in human cancer cells (e.g., breast and ovarian cancer and glioblastoma multiforme; refs. 14–16).

We used both a descriptional and a functional approach to clarify the role of vitamin D_3 metabolism in glioblastoma multiforme.

Materials and Methods

Tumor tissues. Tumor samples were kindly provided by the Department of Neurosurgery and were used with consent of the patients. All tumor samples originated from grade 4 glioblastoma multiforme, as determined by the Department of Neuropathology (Homburg, Germany).

Cell culture. COS-1 cells and rat glioblastoma multiforme cell line C6 were purchased from the American Type Culture Collection (Manassas, VA). Cell lines TX3868 and TX3095 were established from glioblastoma and xenografted on mice. The remaining glioblastoma multiforme cell lines were established from cytologic diagnosed glioblastoma multiforme without xenografting. All glioblastoma multiforme cell cultures were maintained in DMEM/Ham's F12 (DMEM/F12) medium (Invitrogen, Karlsruhe, Germany) supplemented with 1 μg/L penicillin/streptomycin (PAA, Coelbe, Germany) and 10% FCS (PAA). Cells were transferred to serum-free DMEM/F12 medium containing the following additives: 1 μg/L penicillin/streptomycin, 1× insulin/transferrin/selenium (ITS-X, Invitrogen), and 1% bovine serum albumin (Sigma, Taufkirchen, Germany) 24 hours before enzyme assays. The following media were used for proliferation assays: serum-free medium as described above or serum-reduced medium DMEM/F12 supplemented with penicillin/streptomycin, ITS-X, bovine serum albumin, and 2% charcoal/dextran-treated FCS (HyClone, Erembodegem-Aalst, Belgium).

Isolation of total RNA and mRNA, reverse transcription-PCR, and nested touchdown reverse transcription-PCR. Isolation of total RNA and mRNA, classic reverse transcription-PCR (RT-PCR), and nested touchdown RT-PCR from tissues and cell culture were done as described previously (12, 17). Normal brain RNA was obtained from Clontech (Palo Alto, CA).

Real-time reverse transcription-PCR. Real-time RT-PCR was carried out using a Light Cycler (Roche Diagnostics, Mannheim, Germany) by measuring the binding of the fluorescence dye SYBR green I (DNA Master SYBR green I, Roche Diagnostics) to double-stranded DNA. The crossing points (Cp, beginning of the PCR exponential phase) for each reaction were determined by the Second Derivative Maximum algorithm and arithmetic baseline adjustment. We used the RelQuant 1.01 quantification software using the principle of efficiency-corrected calibrator normalized relative quantification. Standard curves were assessed in triplicates and confirmed in two independent experiments (see Supplementary Fig. S1). For quantification, the relative ratio of target gene (*CYP27B1*, *VDR*, *CYP24*) to reference gene (*β_2-microglobulin*) for each sample and for the calibrator was calculated (Cp median, Cpm). The target reference ratio of each sample was then divided by the target reference ratio of the calibrator and corrected for PCR efficiency (ΔCp median, ΔCpm). We determined the variance of ΔCpms for the calibrator of each investigated gene (ΔCp median variance) to show reproducibility.

All PCR reactions were done in duplicate for each cDNA sample. Primer sequences and optimized reaction specificities for each primer pair are given in the Supplementary Table S1. The program was as follows: initial melting for 10 minutes at 95°C, 50 cycles consisting of melting for 10 seconds at 95°C, annealing for 5 seconds at 60/62°C, and elongation for 5 seconds at 72°C with a single fluorescent reading at the end of each cycle. The program was completed with a melting curve analysis. To exclude contamination with DNA, we did Alu-PCR and minus reverse transcriptase control.

PCR and cloning of normal CYP27B1 and splice variants into bacterial and mammalian expression plasmids. The cDNA sequences of the normal enzyme and the splice variants Hyd-V2, Hyd-V3, and Hyd-V4 were generated by RT-PCR as previously described (12). The inserts were amplificated using primers 5′ Hyd (5′-CGGGATCCACCCA-GACCCTCAAGTACG-3′) containing a *Bam*HI restriction site and 3′Hyd Hyd (5′-CCCAAGCTTTAGGGGAAGATGTATACC-3′) containing a *Hin*dIII restriction site (5 minutes 94°C, 1 minute 94°C, 45 seconds 57°C, 1.5 minutes 72°C for 26 cycles, 10 minutes 72°C). PCR products were gel purified and extracted with the QIAquick Gel Extraction Kit (Qiagen, Hilden, Germany). Following *Bam*HI/*Hin*dIII digestion, the inserts were ligated into the pQE-30 expression vector *in frame* to the 6× His-Taq. The recombinant plasmids were transformed in *Escherichia coli* strain M15(pREP4).

The inserts of CYP27B1, Hyd-V2, and Hyd-V4 cloned in pGEM-T Easy were amplified using primers 5′ HydStart (5′-ATGACCCAGACC CTCAAGTACGC-3′) and 3′ HydStop (5′-CTATCTGTCCAAAAACTG-TAGGTTGATGCTC-3′). PCR products were gel-purified and cloned into the mammalian expression vector pcDNA3.1-TOPO (Invitrogen).

Recombinant expression of normal CYP27B1 and three splice variants. Transformed *E. coli* cells were grown in Luria-Bertani medium with kanamycin (25 μg/mL) and ampicillin (100 μg/mL).

Protein expression was induced at an absorbance of 0.6 at 600 nm with isopropyl-L-thio-B-D-galactopyranoside in a final concentration of 1 mmol/L. Samples of the bacterial cultures were obtained before induction and 1, 2, 3, and 4 hours after induction of protein expression by isopropyl-L-thio-B-D-galactopyranoside. Bacterial lysates were subjected to SDS-PAGE and electroblotted onto polyvinylidene difluoride-Membrane (Millipore, Bedford, MA). Expression of the recombinant proteins was shown via detection of the His-Taq with Ni-NTA-Conjugate (Qiagen).

Generation and purification of polyclonal antibodies. The synthesis of three CYP27B1-specific antibodies was carried out using antigenic regions of the reported human amino acid sequence. Two antibodies were generated using peptides located in exon 1 (Ab401, amino acids 1-14, MTQTLKYASRVFHR and Ab461, amino acids 35-48, RSLA-DIPGPSTPS). The peptide for Ab462 is located in exon 5 (amino acids 267-281, HVERREAEAAMRNG). Peptide synthesis, generation, and purification of polyclonal antibodies were done as described previously (18). Protein lysates from tissue samples and cell cultures were prepared as described previously (18, 19).

Western blot of tissue and cell culture lysates. Proteins were subjected to 12.5% SDS-PAGE and transferred to polyvinylidene difluoride membranes (Millipore). Filters were blocked and incubated with primary preabsorbed antibody at a final dilution of 1:375. Monoclonal mouse anti-α-tubulin antibody (Sigma) was used in a 1:10,000 dilution. Blocking experiments were with primary antibody preabsorbed with 100-fold excess of immunizing peptide. BLAST-Algorithm

[4] Unpublished data.

was to exclude homology of the used peptides to other cytochrome *P*450. Densitometric analysis was done with BioDocAnalyze (Biometra, Göttingen, Germany).

Measurement of CYP27B1 activity in transfected COS-1 cells and glioblastoma multiforme cell cultures. CYP27B1 activity was determined as described previously (20–23). Glioblastoma multiforme cell cultures were seeded in 60-mm^2 plates at 1.2×10^6 or 1.5×10^6 cells per dish and grown in serum-free medium to 90% confluency. COS-1 cells were seeded in 60-mm^2 plates at 5×10^5 cells per dish in DMEM/F12 containing FCS. Cells were transfected with pcDNA3.1 plasmids as described above with Effectene Transfection Reagent (Qiagen). The general transfection efficiency was 30 ± 2.4% as quantified by fluorescence-activated cell sorting analysis (Becton Dickinson, Heidelberg, Germany). Twenty-four hours after transfection, cells were washed with serum-free medium and incubated with 1 μmol/L 25-(OH)D_3 (Biomol, Hamburg, Germany) and 0.1 μCi/mL [^{3}H]25-(OH)D_3 (187 Ci/mmol, Amersham, Freiburg, Germany) for 4 and/or 24 hours at 37°C. Media and cells were collected for extraction of vitamin D metabolites with methanol/chloroform (1:4, v/v). The extracts were dried, redissolved in 10 μL hexane, and separated on glass-backed silica-coated high-performance TLC (HPTLC) plates (Kieselgel 60 F_{254}, Merck, Darmstadt, Germany) in dichloromethane/isopropanol (9:1, v/v). Standard contained 25-(OH)D_3, [^{3}H]25-(OH)D_3, and 1α,25-$(OH)_2D_3$ (Biomol). Conversion of tritiated 25-(OH)D_3 was quantified after exposure to Fuji imaging plates using a phosphoimager (BAS-250, Fuji, Stamford, CT). Nonradioactive standards were made visible using UV light. All data were calculated from three independent experiments, each done in duplicates and were normalized against equal cell numbers.

Calcitriol/calcidiol treatment of cell cultures. If not mentioned otherwise, cells were seeded for proliferation assays at 1,000 cells per well into 96-well plates. After 12 hours, cells were maintained 24 hours in serum-free or serum-reduced DMEM/F12. Calcitriol was added in concentrations ranging from 10^{-12} to 10^{-6} mol/L and calcidiol in a dose of 2.5×10^{-8} mol/L. Cells treated with solvent (ethanol) were included as controls. The medium was replaced every other day containing fresh vitamin D_3 metabolites. After 6 days (144 hours), cell proliferation was determined using WST-1 Reagent (Roche Diagnostics) after manufacturers' instructions.

For real-time PCR, cells were seeded at 6.4×10^6 cells per well into 100-mm^2 plates. Subconfluent cells were washed and cultured for 24 hours in serum-free medium. Cells were treated with 10^{-8} mol/L calcitriol dissolved in ethanol or with solvent alone for 16 hours followed by a calcitriol-free incubation period of 32 hours. Forty-eight hours after treatment, cells were collected and RNA was isolated as described previously.

Results

New splice variants of CYP27B1 in glioblastoma multiforme. We recently reported several new splice variants of CYP27B1 mRNA (17). After cloning further variants from the glioblastoma multiforme cell line TX3868 (Fig. 1), we sequenced 16 splice variants including variant Hyd-V3 with deletion of a part of exon 8; variant Hyd-V2 with deletion of the entire exons 4 and 5; two variants Hyd-V1 and Hyd-V7 with deletion of exons and insertion of introns, respectively; variant Hyd-V4 with insertion of a part of intron 2; and variants Hyd-V5, Hyd-V6, Hyd-V8 to Hyd-V16 with insertions of one or several entire introns. The majority of the sequence variations results in frameshifts and premature termination signals. The only variant retaining the heme-binding and the ferredoxin-binding sites is Hyd-V4, containing a 27 AS in-frame insertion of intron 2. Northern blot analysis of glioblastoma multiforme cell line TX3868 identified two signals at 2.0 and 4.0 kb corresponding

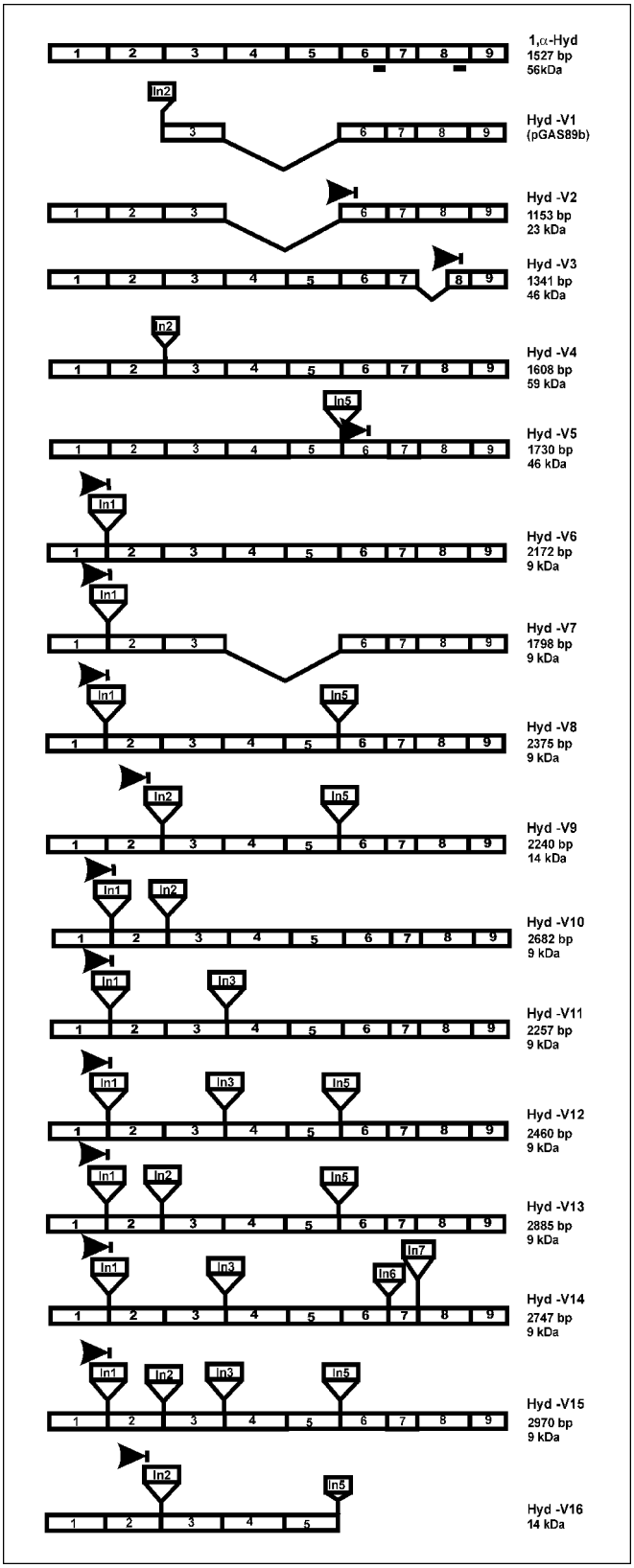

Fig. 1. Organization of the normal and the alternatively spliced CYP27B1 mRNAs. *Heavy bars*, coding regions for the ferredoxin-binding site in exon 6 and for the heme-binding site in exon 8, respectively. *Arrows*, premature stop codons. Sizes of the open reading frames without 5′ untranslated regions (62 bp) and 3′ untranslated regions (806 bp) are indicated in bp and sizes of potential resulting proteins are indicated in kDa.

in size to variant Hyd-V2 (2,085 bp) and to variant Hyd-V15 (3,904 bp; data not shown).

Metabolism of calcidiol by CYP27B1 and splice variants. We determined the percentile production of calcitriol in transfected COS-1 cells. We selected Hyd-V4, the only variant containing the functional domains necessary for enzymatic activity and Hyd-V2, as an example for the remaining splice variants with deletions of functional domains. The latter splice variants are not likely to have any enzymatic activity. We subcloned the coding sequences of the normal CYP27B1 (1α-Hyd) and the splice variants Hyd-V2 and Hyd-V4 into pcDNA3.1 and expressed them in mammalian COS-1 cells. The cDNA of Hyd-V4 was also cloned in reverse orientation to serve as control. RT-PCR confirmed the expression of the corresponding mRNAs in the transfected cells. HPTLC separation of tritiated calcidiol was used to determine the relative percentile production of calcitriol over a 4-hour incubation period. HPTLC analysis of COS-1 cells transfected with control vector showed a peak at 49 mm coincident with authentic calcidiol standard. COS-1 cells transfected with pcDNA3.1/1α-Hyd showed peaks at 49 and 21 mm coincident with authentic calcidiol and calcitriol standards (Fig. 2A). In COS-1 cells transfected with the normal CYP27B1 cDNA sequence, there was a mean 14.2% conversion from calcidiol to calcitriol (Fig. 2B). COS-1 cells transfected with splice variants Hyd-V2 and Hyd-V4 showed no higher CYP27B1 activity than control cells transfected with Hyd-V4 in reverse orientation. An elevated incubation period of 24 hours revealed similar results (data not shown). Additionally, peaks at 11 and 36 mm were detected, that were referred to in Discussion.

Quantification of CYP27B1 expression in glioblastoma multiforme biopsies and cell cultures. We assessed the expression of the *CYP27B1* gene relative to the housekeeping gene *β_2-microglobulin* by real-time RT-PCR using primers from exon 1 of the *CYP27B1* gene. We analyzed glioblastoma multiforme biopsies with and without gene amplification, glioblastoma multiforme cell cultures with and without amplification, and a normal human brain sample (Table 1). A 2-fold increase of gene expression in comparison with normal brain was considered as elevated expression. CYP27B1 expression was elevated in 8 of 10 tumor biopsies with gene amplification (80%), in 4 of 10 tumor biopsies without gene amplification (40%), in 5 of 5 cell lines with gene amplification (100%), and in 4 of 5 cell lines without gene amplification (80%). In total, 12 of 20 glioblastoma multiforme biopsies and 9 of 10 glioblastoma multiforme cell cultures showed an elevated gene expression in comparison to normal human brain. Furthermore, a clear increase of CYP27B1 expression was detected in five of six cell cultures in comparison with the corresponding primary tumor sample (H246, H366, H545, H546, and H556).

Antibodies against CYP27B1 and variants of CYP27B1. We generated antibodies Ab401 and Ab461 for the detection of all CYP27B1 variants using peptides located in exon 1. Additionally, we generated antibody Ab462 using a peptide located in exon 5 (4). We tested the specificity of the CYP27B1 antibodies using CYP27B1 wild type protein and the splice variants Hyd-V2, Hyd-V3, and Hyd-V4, all of them expressed as 6× His fusion proteins in *E. coli*. The expression of the recombinants was confirmed with a Ni-NTA-conjugate (see Supplementary Fig. S2). The purified antibodies Ab401 and Ab461 identified all four recombinant proteins including the normal protein at 56 kDa, the variant Hyd-V2 at 23 kDa, the variant Hyd-V3 at 49 kDa, and the variant Hyd-V4 at 59 kDa. Antibody Ab462 detected the normal CYP27B1 recombinant protein and the variants Hyd-V3 and Hyd-V4 but not the variant Hyd-V2 that shows a deletion of exons 4 and 5. These results are consistent

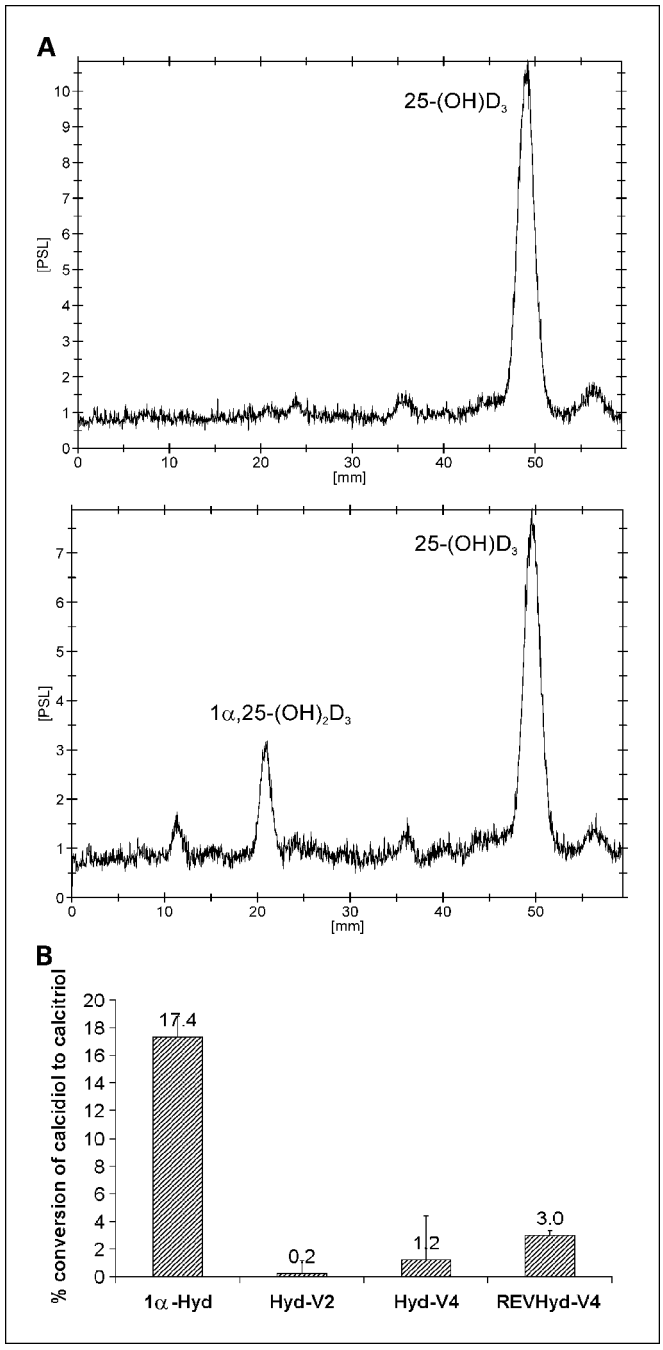

Fig. 2. Metabolism of calcidiol in transfected COS-1 cells. Cells were transfected with the mammalian expression vector pcDNA3.1-TOPO with different cDNA inserts including normal CYP27B1 (1α-Hyd), splice variant Hyd-V2, and splice variant Hyd-V4. Recombinant pcDNA3.1-TOPO with Hyd-V4 in reverse orientation (REVHyd-V4) served as a control. After 24 hours, cells were incubated with calcidiol for 4 hours. *A*, HPTLC analysis of radiolabeled vitamin D metabolites in COS-1 cells transfected with pcDNA3.1/REVHyd-V4 (*top*) and with pcDNA3.1/N-Hyd (*bottom*). PSL, photostimulated luminescence. *B*, CYP27B1 activity of transfected COS-1 cells. The data that represent means from duplicate assays are shown as the percent conversion of [^{3}H]25-(OH)D_3 (calcidiol) to [^{3}H]1α,25-$(OH)_2D_3$ (calcitriol).

with the localization of the peptides used to generate the antibodies (see Supplementary Fig. S3).

Additional control experiments on glioblastoma multiforme protein lysates were done with antibodies preabsorbed with 100× immunizing peptide and with preimmune sera (see Supplementary Fig. S4).

CYP27B1 protein in glioblastoma multiforme biopsies and glioblastoma multiforme cell cultures. Using Western blotting, we analyzed the expression of the *CYP27B1* gene in 15 glioblastoma multiforme biopsies, two glioblastoma multiforme cell cultures, and three normal human tissues including brain. All antibodies detected a signal at 56 kDa that corresponds to the size of the normal CYP27B1 protein. We also identified additional signals that likely represent splice variants. The predicted protein sizes of the known variants correspond to the sizes of the proteins detected by Western blot analysis. Antibody Ab401 identified proteins at 14.1 kDa likely representing Hyd-V1, Hyd-V9, and Hyd-V16. Antibody Ab461 identified proteins at 22.7 kDa likely representing variant Hyd-V2. Both antibodies identified proteins at 45.5 and 46 kDa likely representing Hyd-V3 and Hyd-V5, respectively, and a protein at 58.9 kDa likely representing Hyd-V4. The variants containing an insertion of intron 1 were not represented by a protein of the corresponding size (9.2 kDa). Antibody Ab462 identified proteins at sizes between 45 and 75 kDa likely representing splice variants Hyd-V3, Hyd-V4, and Hyd-V5 and the normal enzyme. Additionally, all three antibodies detected proteins that are larger than the expected protein sizes (Fig. 3A-C).

The antibodies detected minor differences in the intensity of specific bands. Single differences as for example the increased intensity of the 56-kDa band in sample H205 likely depend on different sensitivity of the antibodies and will not be addressed in detail (Fig. 3A). In general, antibodies Ab401 and Ab461 identified a similar overall expression pattern in glioblastoma multiforme biopsies and

Table 1. Expression analysis of CYP27B1, VDR, and CYP24 employing real-time PCR

Origin	Sample	CYP27B1		VDR		CYP24	
		RQV	RQV sample/RQV brain	RQV	RQV sample/RQV brain	RQV	RQV sample/RQV brain
Biopsy	H91 (+)*	2.1e −03	1.8e+00	2.1e −03	3.9e−02	2.0e−03	2.2e+01
	H220 (+)	2.2e−03	1.9e+00	8.0e−04	1.5e−02	5.7e−03	6.4e+01
	H246 (+)*	4.7e−03	4.1e +00	3.7e−03	7.0e−02	1.9e−03	2.1e+01
	H346 (+)	3.1e −02	2.8e+01	1.9e−02	3.6e−01	0.0e+00	0.0e+00
	H385 (+)*	2.8e−03	2.4e+00	4.1e −03	7.7e−02	0.0e+00	0.0e+00
	H549 (+)	1.1e −02	9.8e+00	9.1e −03	1.7e−01	5.5e−04	6.1e+00
	H552 (+)	2.1e −01	1.8e+02	3.9e−03	7.4e−02	2.3e−04	2.5e+00
	H556 (+)	3.1e −03	2.7e+00	3.0e−03	5.6e−02	9.6e−05	1.1e +00
	H570 (+)	3.5e−03	3.1e +00	0.0e +00	0.0e+00	0.0e+00	0.0e+00
	H981 (+)	1.1e −02	9.9e+00	1.3e−02	2.5e−01	3.3e−03	3.6e+01
	H49 (−)	8.2e−03	7.2e+00	1.3e−03	2.5e−02	3.6e−03	4.1e +01
	H226 (−)	2.5e−02	2.2e+01	0.0e+00	0.0e+00	4.5e−04	5.0e+00
	H281 (−)	3.2e−02	2.9e+01	0.0e+00	0.0e+00	0.0e+00	0.0e+00
	H282 (−)*	1.3e−01	1.1e +02	5.0e−03	9.5e−02	0.0e+00	0.0e+00
	H321 (−)	5.5e−05	4.8e−02	2.9e−04	5.5e−03	2.0e−03	2.3e+01
	H323 (−)	1.6e−03	1.4e+00	0.0e+00	0.0e+00	1.3e−02	1.5e+02
	H361 (−)*	6.1e −04	5.4e−01	2.0e−03	3.8e−02	0.0e+00	0.0e+00
	H366 (−)*	1.2e−03	1.1e +00	4.5e−01	8.5e+00	0.0e+00	0.0e+00
	H545 (−)	8.4e−04	7.4e−01	3.4e−03	6.5e−02	1.7e−02	1.9e+02
	H546 (−)	1.1e −03	9.6e−01	7.6e−04	1.4e−02	5.4e−05	6.0e−01
Cell line	T3868 (+)	1.6e−02	1.5e+01	3.3e−03	6.3e−02	1.5e−04	1.7e+00
	TX3868 (+)*	6.8e−02	6.0e+01	5.4e−03	1.0e−01	0.0e+00	0.0e+00
	H246 (+)	2.2e−02	1.9e+01	1.1e −03	2.2e−02	6.8e−03	7.6e+01
	H346 (+)	1.3e−02	1.1e +01	1.3e−04	2.5e−03	0.0e+00	0.0e+00
	H556 (+)	1.3e+00	1.2e+03	0.0e+00	0.0e+00	1.7e−05	1.9e−01
	T3095 (−)	2.9e−03	2.5e+00	1.3e−04	2.5e−03	0.0e+00	0.0e+00
	TX3095 (−)	4.7e−04	4.1e−01	3.5e−04	6.7e−03	0.0e+00	0.0e+00
	H366 (−)	2.5e−01	2.2e+02	0.0e+00	0.0e+00	0.0e+00	0.0e+00
	H545 (−)	5.9e−02	5.2e+01	2.8e−03	5.3e−02	0.0e+00	0.0e+00
	H546 (−)	2.5e−02	2.2e+01	1.5e−02	2.8e−01	0.0e+00	0.0e+00
Biopsy	Brain	1.1e −03	1	5.3e−02	1	9.0e−05	1

NOTE: Values provided represent means from duplicate assays from the same sample. (+), amplification of the CYP27B1 gene.(−), absence of amplification. RQV, relative quantification value.

*CYP27B1 expression previously analyzed employing conventional RT-PCR (12).

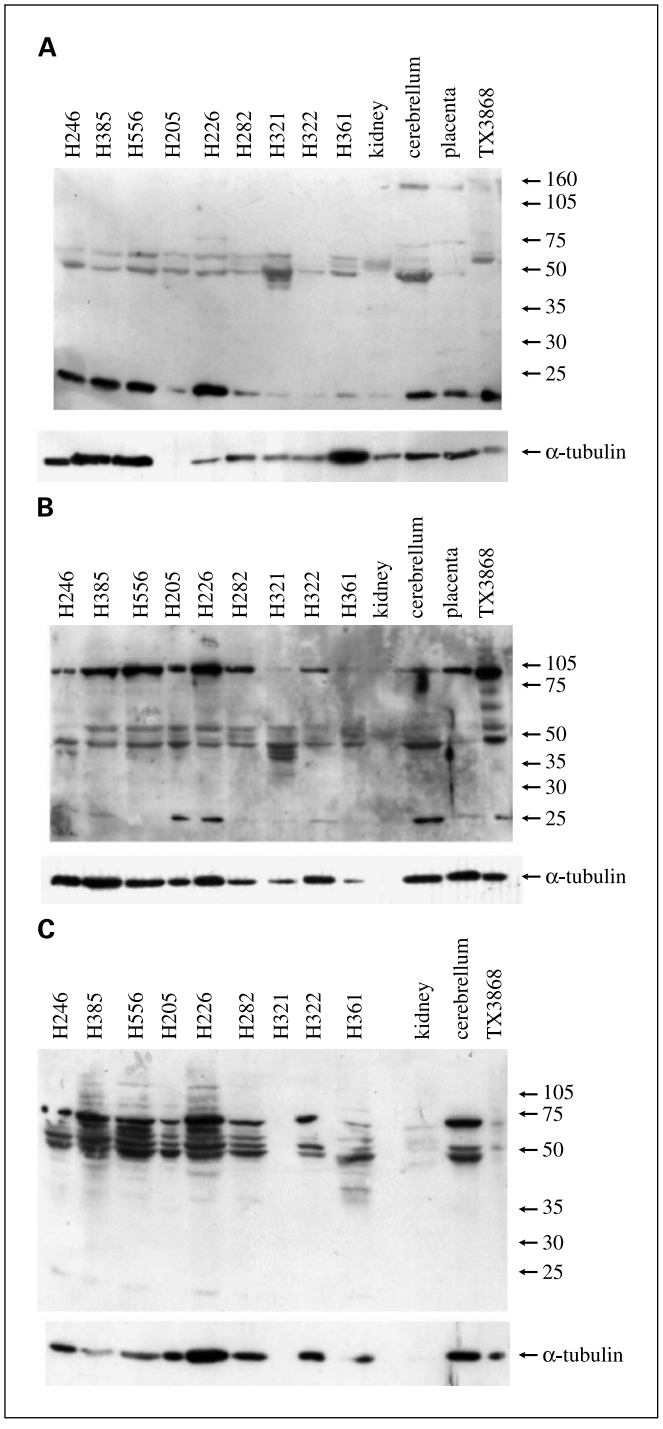

Fig. 3. Immunologic detection of CYP27B1 (56 kDa) and potential splice variants with CYP27B1 specific antibodies Ab401 (*A*), Ab461 (*B*), and Ab462 (*C*) in different total protein lysates of glioblastoma multiformes and normal tissues. (+), amplification of the *CYP27B1* gene; (−), absence of amplification. Positions and sizes (kDa) of molecular mass markers (*right*). The membranes were reprobed with α-tubulin mouse antibody (*bottom*).

glioblastoma multiforme cell cultures but a slightly different expression pattern in normal tissues. Antibody 462 identified an expression pattern different from the pattern found by the antibodies Ab401 and Ab461. However, antibody Ab462 confirmed the similarity of the expression pattern among glioblastoma multiforme biopsies found by the antibodies Ab401 and Ab461. Likewise, antibody Ab462 confirmed the difference between the expression pattern of glioblastoma multiforme samples and normal tissues. Using anti-tubulin antibody for normalization, we did densitometric analysis of CYP27B1 protein in glioblastoma multiforme biopsies. Although the intensity of single bands was different in some cases, antibodies 401, 461, and 462 did not reveal major differences in the overall expression pattern. In summary, our analysis of the normal CYP27B1 protein and its variants showed an expression profile that is (i) similar among glioblastoma multiformes, (ii) different between glioblastoma multiformes and normal human tissues, and (iii) unrelated to the *CYP27B1* gene amplification status.

CYP27B1 activity in glioblastoma multiforme cell cultures. We tested glioblastoma multiforme cell cultures for CYP27B1 activity by analyzing the conversion of calcidiol. The conversion was normalized against plates without cells to exclude possible background oxidation of calcidiol. In total, we analyzed nine glioblastoma multiforme cell cultures including five glioblastoma multiforme cell cultures with *CYP27B1* gene amplification and four cell cultures without gene amplification. We also included the human glioblastoma multiforme cell line U373 and rat C6 cell line with unknown amplification status of the *CYP27B1* gene. The relative percentile production of radiolabeled metabolites of calcidiol was determined over a 4-hour incubation period. A typical HPTLC separation of tritiated calcidiol metabolism in medium alone and in glioblastoma multiforme cells is shown in Fig. 4A. A product peak at 49 mm was coincident with authentic calcidiol standard, whereas the peak of a more polar enzymatic product at 23 mm slightly differed to authentic calcitriol, showing a peak at 21 mm. All glioblastoma multiforme cell cultures showed conversion from calcidiol to this unidentified metabolite with a mean value of 3.5% (Fig. 4B). In detail, the glioblastoma multiforme cell lines with *CYP27B1* gene amplification showed a mean conversion value of 2.9% with a low SD and the glioblastoma multiforme cell lines without gene amplification showed a mean conversion value of 4.1% with a higher SD. An extended incubation time of 24 hours resulted in similar results (data not shown).

Effect of calcitriol and calcidiol on glioblastoma multiforme cell lines. We examined the effect of calcitriol on cell proliferation in nine human glioblastoma multiforme cell lines and rat glioblastoma multiforme cell line C6. Melanoma cell line MeWo, known as sensitive for calcitriol (24), served as control. We confirmed a growth inhibition of 56.3 ± 8.8% in the latter cell line by 10^{-7} mol/L calcitriol. Glioblastoma multiforme cell lines were cultivated in serum-free medium, unless insufficient proliferation required the use of serum-reduced medium. For C6 cells cultured in serum-free medium, a cell density–specific effect was detectable. Seeding 400 cells, there was a dose-dependent growth inhibition by calcitriol. In contrast, seeding 800 cells, there was a proliferative effect of calcitriol at all concentrations. The proliferative effect was maximal at low doses (10^{-10} mol/L; Fig. 5A).

Glioblastoma multiforme cell line TX3868 in serum-free medium showed a comparable proliferative calcitriol effect in several doses. There was no significant effect detectable in three

other glioblastoma multiforme cell lines (H346, H366, and TX3095; Fig. 5B). In serum-reduced medium, TX3868 also showed a proliferative response to calcitriol at a low dose (10^{-10} mol/L). A high dose of calcitriol caused a proliferation of TX3095. The other cell lines did not show significant dose-dependent effects of calcitriol. (Fig. 5C).

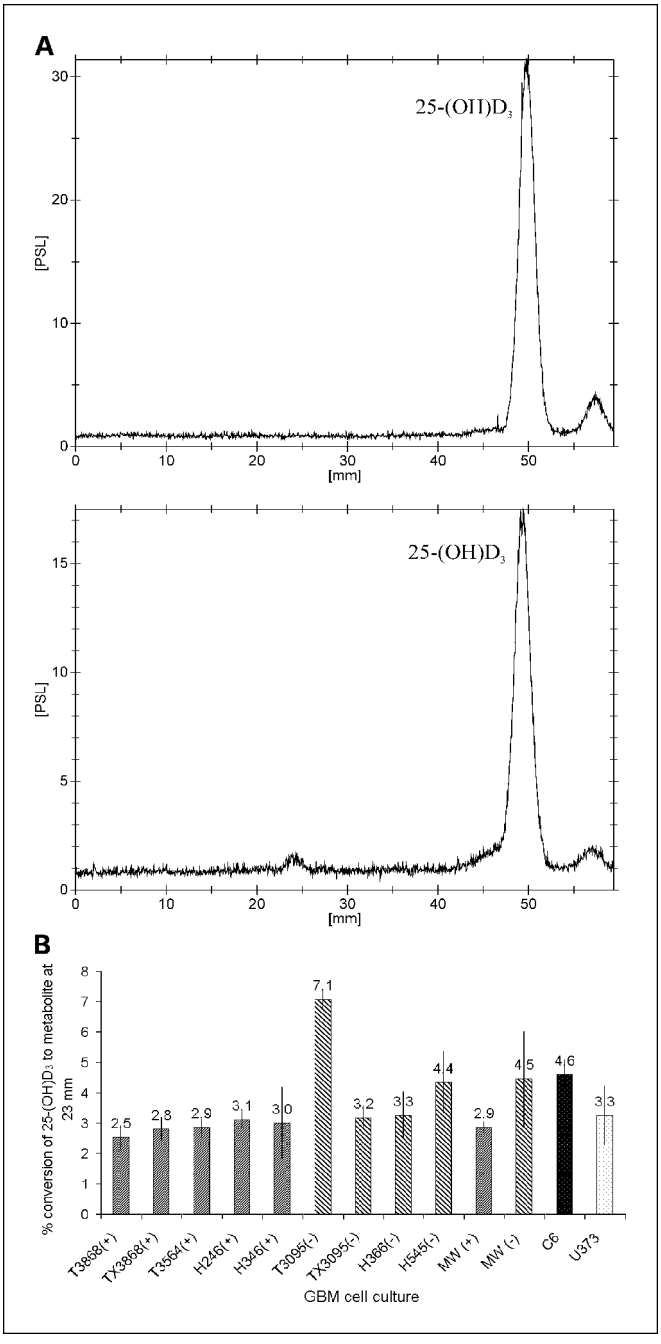

Fig. 4. Analysis of calcidiol metabolism in glioblastoma multiforme cell lines. Cells were incubated 24 hours in serum-free medium before adding calcidiol for 4 hours. *A*, HPTLC analysis of radiolabeled vitamin D metabolites of medium without cells (*top*) and of glioblastoma multiforme cells (*bottom*). PSL, photostimulated luminescence. *B*, CYP27B1 activity in nine human glioblastoma multiforme cell lines and rat C6 cells. Data are normalized against cell number and are shown as the percent conversion of [^{3}H]25-(OH)D_3 (calcidiol) to the unidentified, tritiated metabolite minus the control (medium alone). (+), amplification of the *CYP27B1* gene; (−), absence of amplification. *Columns*, means from duplicate assays.

An analogue treatment with 2.5×10^{-8} mol/L calcidiol resulted in a proliferative effect on C6 cells cultivated in serum-free medium and seeded at a density of 400 or 800 cells per well. Likewise, we found a proliferative effect for cell culture TX3095 also cultivated in serum-free medium. Cell culture H366 did not show an effect, and cell cultures H346 and TX3868 showed a low antiproliferative effect (Fig. 5D). In serum-reduced medium, we found a proliferative effect of calcidiol in three of nine glioblastoma multiforme cultures and an antiproliferative effect in the remaining six glioblastoma multiforme cell cultures (Fig. 5E).

Quantification of vitamin D receptor and CYP24 expression in glioblastoma multiforme biopsies and cell cultures. We quantified the mRNA expression of the *VDR* gene and the *CYP24* gene in glioblastoma multiforme biopsies and glioblastoma multiforme cell cultures that were used for quantification of CYP27B1. The expression of the genes was normalized against the housekeeping gene *β_2-microglobulin* (Table 1) and compared with normal brain.

Real-time RT-PCR showed higher mRNA expression of the *VDR* gene in normal brain than in glioblastoma multiforme biopsies and cell cultures, including glioblastoma multiformes without detectable VDR expression. Out of 20 tumors, only tumor H366 showed a higher expression of the *VDR* gene in comparison with normal brain (8.5-fold). For the other 19 glioblastoma multiforme biopsies, the expression of the *VDR* gene was 13.8-fold lower than in normal brain. There was no significant difference in the expression level of the *VDR* gene between tumors with and tumors without 12q13-14 gene amplification of *CYP27B1*. Cultures including H366 showed a low expression level of the *VDR* gene in comparison to normal brain (18.8-fold), with two cell lines lacking any detectable VDR expression.

Real-time RT-PCR showed a strong CYP24 expression in 13 of 20 glioblastoma multiforme biopsies (43-fold higher than in normal brain). In seven biopsies, no expression was detectable. Out of 10 glioblastoma multiforme cell cultures, only culture H246 showed a significant CYP24 expression (76-fold higher than in normal brain). Both, biopsies and cell cultures, showed no correlation between expression of CYP24 and the amplification status of the *CYP27B1* gene.

Influence of calcitriol on CYP27B1, VDR, and CYP24 expression. Glioblastoma multiforme cell line T3868, carrying a *CYP27B1* gene amplification, was treated with 10^{-8} mol/L calcitriol. The expression of CYP27B1, CYP24, and VDR was determined after 24 hours employing real-time RT-PCR.

The expression of CYP27B1 was elevated 4.9 times after calcitriol treatment in comparison to the solvent control (Fig. 6). The expression of the VDR was not significantly increased in comparison with normal brain. Treatment of T3868 with 10^{-8} mol/L calcitriol revealed a 24.7-fold elevated expression of CYP24 in comparison with normal brain. By contrast, in cells treated with vehicle alone no CYP24 expression was detectable.

Discussion

This study contributes to a more complete picture of CYP27B1 variants in glioblastoma multiforme. A majority of splice variants, including Hyd-V6 to Hyd-V8 and Hyd-V10 to Hyd-V15, contain intron 1. These splice variants and splice

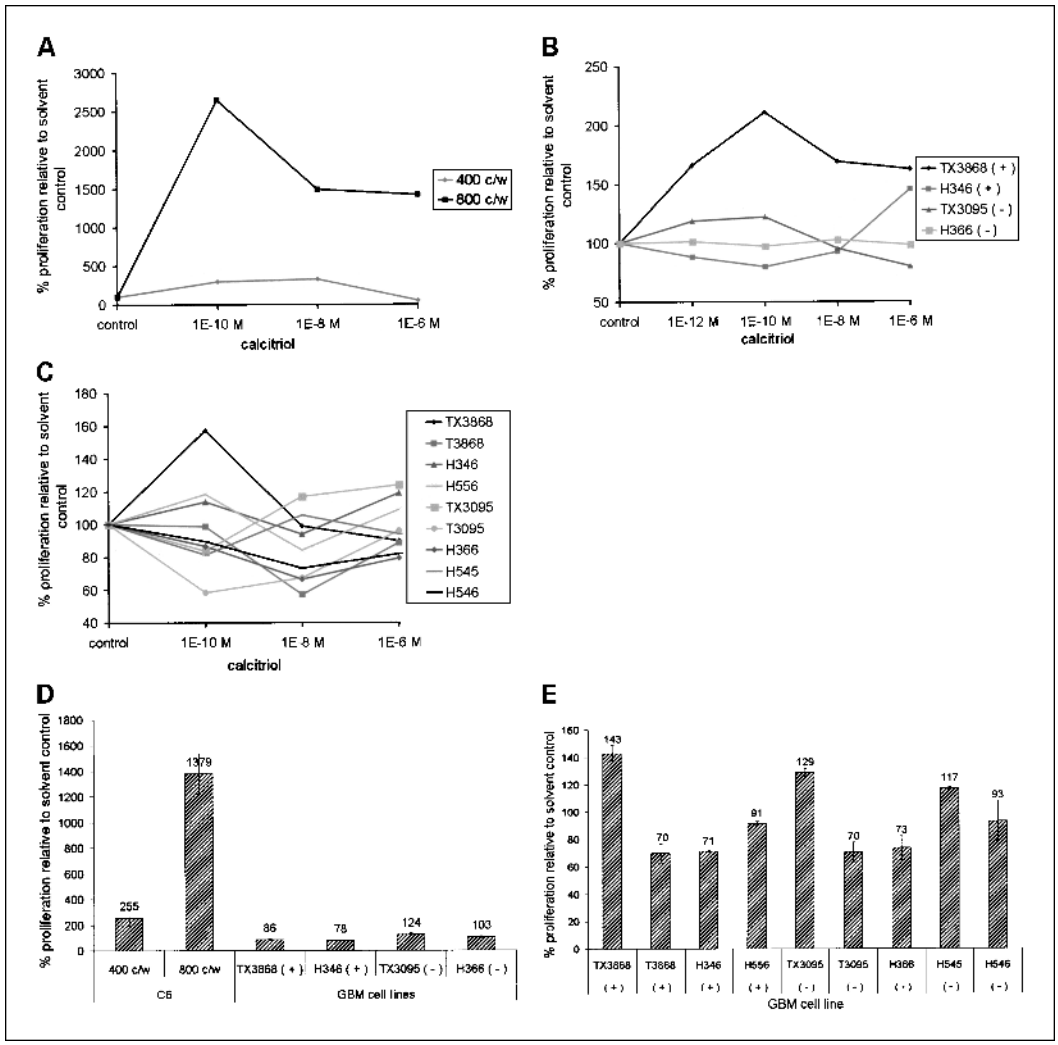

Fig. 5. Effect of $1\alpha,25\text{-}(OH)_2D_3$ (calcitriol) and $25\text{-}(OH)D_3$ (calcidiol) on the proliferation of glioblastoma multiforme (*GBM*) cell lines determined by WST-1 assay. Cells were exposed to the indicated doses of vitamin D_3 metabolites every other day over a total time of 6 days. Proliferation was normalized against the respective solvent control (100 %). *A*, calcitriol treatment of rat C6 cells grown in serum-free medium. *B*, calcitriol treatment of human glioblastoma multiforme cell lines grown in serum-free medium. *C*, calcitriol treatment of human glioblastoma multiforme cell lines grown in serum-reduced medium. *D*, calcidiol treatment of rat C6 cells and human glioblastoma multiforme cell lines grown in serum-free medium *E*, calcidiol treatment of human glioblastoma multiforme cell lines grown in serum-reduced medium. (+), amplification of the *CYP27B1* gene; (−), absence of amplification; c/w, cells seeded per well.

variants Hyd-V2, Hyd-V3, Hyd-V5, Hyd-V9, and Hyd-V16 result in truncated proteins with deletions of protein domains essential for enzymatic activity, including oxygen-, hormone-, heme-, and ferredoxin-binding sites (25, 26). In agreement with these data, we did not find enzymatic activity in COS-1 cells expressing Hyd-V2. In addition, we did not find residual enzymatic activity in COS-1 cells expressing variant Hyd-V4, which contains domains essential for enzymatic activity but shows an in-frame insertion of 27 AA of intron 2. This insertion may confound the enzymes' conformation and therefore its activity.

These findings leave the question about the biological meaning of the alternative splicing of CYP27B1. A shift to the expression of splice variants followed by nonsense-mediated mRNA decay might cause a lower expression level of mRNA coding the active enzyme (27). However, we found that the majority of CYP27B1 splice variants is not degraded on RNA level but likely exists as proteins without enzymatic activity. The expression of CYP27B1 may be a steady state of fine-tuned equilibrium of stable and unstable mRNAs and active and inactive protein products. In this context, the expression of a wide variety of inactive CYP27B1 protein variants may imply a reduction in the relative amount of active enzyme.

CYP27B1 is ubiquitously expressed in extrarenal cells (4) and the pattern of regulation of CYP27B1 expression differs between kidney and extrarenal cells (6). In this and in previous studies, we report specific CYP27B1 mRNA variants in normal and in tumor tissues (12, 17, 28). The newly generated antibodies detected similar patterns among glioblastoma multiformes and different patterns between glioblastoma multiformes and normal human tissues, indicating a tissue-specific mode of CYP27B1 expression. Such a tissue-specific expression pattern has been suggested as prominent sign for the role of alternative splicing as regulation mechanism (29).

To evaluate the biological meaning of *CYP27B1* gene amplification in glioblastoma multiforme, we determined the mRNA and protein expression levels. We found an elevated mRNA expression in glioblastoma multiforme biopsies with gene amplification in contrast to tumors without gene amplification. Western blot experiments did not confirm an elevated expression in glioblastoma multiforme biopsies with gene amplification. This inconsistency may reflect a cellular mechanism that levels out mRNA expression differences that were due to amplification. Alternatively, this inconsistency may be caused by different sensitivity of the quantification methods.

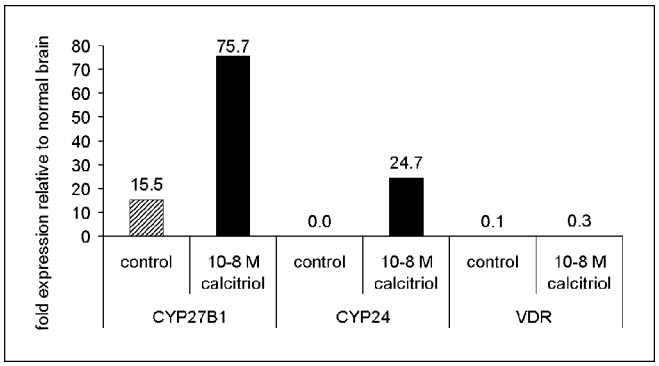

Fig. 6. Expression analysis of CYP27B1, VDR, and CYP24 by real-time RT-PCR after treatment of human glioblastoma multiforme cell line T3868 with 10^{-8} mol/L calcitriol. Cells were cultured in serum-free medium 24 hours before adding calcitriol or solvent alone for 16 hours. After 32 hours, cells were collected for RNA-extraction. *Columns*, means from duplicate assays from the same sample.

The CYP27B1 mRNA expression was elevated in the majority of glioblastoma multiforme cell cultures in comparison with the corresponding tumor biopsy. This difference may be in part explained by the high heterogeneity of glioblastoma multiforme tissues in comparison to cell cultures that are less heterogeneous due to clonal selection (30). Selective pressure in favor of an elevated CYP27B1 expression in glioblastoma multiforme cell cultures may indicate a potential significance of CYP27B1 activity for neoplastic growth in glioblastoma multiforme.

Recently, the 3-epimerization of calcidiol was shown in various cultured cells, including *osteosarcoma*, colon *adenocarcinoma*, and *hepatoblastoma* cells. In addition, it was shown that 3-epi-25-$(OH)D_3$ is metabolized by CYP27B1 to 3-epi-1α,25-$(OH)_2D_3$ (31). The 3-epimere of calcitriol is known to be more stable than calcitriol but to have lower antiproliferative and differentiation inducing activity for various cell lines (31–34). This decrease in biological activity can be explained by a reduced binding affinity to the VDR (31, 33, 35). The conversion to this metabolite has been reported to be tissue specific and to depend on the degree of proliferation (33, 36). The mobility of the unidentified metabolite of calcidiol with a peak at 23 mm may possibly indicate a 3-epimere of calcitriol in glioblastoma multiforme cell lines. The possible formation of 3-epi-calcitriol would in turn indicate CYP27B1 activity in glioblastoma multiforme cell lines. However, final proof of a 3-epimere of calcitriol requires experiments that show comigration of standard 3-epi-1α,25-$(OH)_2D_3$.

Besides the peak at 21 mm corresponding to calcitriol, CYP27B1-transfected COS-1 cells show further peaks likely resulting from the conversion of calcidiol in COS-1 cells. These peaks may correspond to 24,25-$(OH)_2D_3$ (36 mm), 3-epi-1α,25-$(OH)_2D_3$ (23 mm), and 1α,24,25-$(OH)_3D_3$ (11 mm) and thus possibly indicate a background CYP24 activity in COS-1 cells and an active vitamin D_3 metabolism, which would be expected for a renal cell line. The small peaks at 21 mm in untransfected cells and in COS-1 cells transfected with control vector may be due to endogenous CYP27B1 activity or to possible oxidation of calcidiol to 19-nor-10-oxo-25$(OH)D_3$. It is conceivable that these processes occur in all samples.

It is well known that calcitriol can both inhibit and stimulate growth of normal and tumor cells. These effects have been reported to be dependent on the doses of calcitriol and on the presence of growth factors in the culture medium (8, 37). Calcitriol can induce glioma cell death in a dose-dependent manner in rat glioma cell line C6 (38, 39) and in human *glioblastoma* cell lines (40) but not in primary astrocytes (41). Calcitriol sensitivity varies between different glioblastoma multiforme cell cultures (42). We confirmed the antiproliferative mode of action of calcitriol at high doses (10^{-6} mol/L) in C6. We showed that calcitriol can have a proliferative effect at low doses (10^{-10} mol/L) in these cells. Whereas the majority of human glioblastoma multiforme cell lines were calcitriol insensitive, we also found a few cell lines exhibiting a proliferative response to calcitriol treatment, providing first evidence for a mitogenic effect of calcitriol on glioblastoma multiforme cell lines.

It has been previously reported that incubation of prostate cancer cells with calcidiol has the same antiproliferative effect as calcitriol (43). It is possible that the formation of calcitriol from calcidiol may be involved in the calcidiol-mediated effects. Magrassi et al. suggested an antiproliferative effect of calcidiol on glioblastoma multiforme cells (40). We treated a subset of glioblastoma multiforme cell lines with a dose of 2.5×10^{-8} mol/L calcidiol. Like for calcitriol, we also found antiproliferative and proliferative effects of calcidiol. The effects of calcidiol may be mediated by calcidiol itself or by vitamin D_3 metabolites that are derived from calcidiol, as discussed by Lou et al. for prostatic stromal cells (44).

Several classic vitamin D_3 modes of action are described to be mediated through VDR-dependent transcriptional regulation. The mRNA expression of the *VDR* gene in glioblastoma multiforme biopsies and glioblastoma multiforme cell cultures was very low or undetectable in comparison to normal brain. Treatment of glioblastoma multiforme cell culture T3868 with 10^{-8} mol/L calcitriol did not reveal a significant increase in VDR expression. We found, however, a dose-dependent proliferative calcitriol effect on glioblastoma multiforme cell lines. The lack of significant VDR expression in glioblastoma multiforme cell lines indicates other pathways to play a role in vitamin D_3 metabolite–mediated effects on cell growth. Baran et al. hypothesized a membrane receptor responsible for fast nongenomic vitamin D_3 metabolites signaling (45). Magrassi et al. and Elias et al. proposed a receptor specific for vitamin D_3 compounds with low affinity to the nuclear VDR (46, 38).

Of the glioblastoma multiforme biopsies, 65% of samples show expression of CYP24, known to be regulated by calcitriol (47), indicating an active 24-hydroxylation pathway in glioblastoma multiforme, probably depending on the calcitriol level in these tumors. By contrast, in the majority of glioblastoma multiforme cell cultures, we did not find significant CYP24 expression. This may be due to a low calcitriol concentration in culture medium, a notion that is supported by the observation that the addition of 10^{-8} mol/L calcitriol to the culture medium resulted in an induction of *CYP24* gene expression in T3868.

Several studies reported a resistance of CYP27B1 gene expression to the negative regulatory effects of calcitriol for cells derived from extrarenal sites (48, 49). Calcitriol treatment of glioblastoma multiforme cell culture T3868 carrying a CYP27B1 amplification resulted in an increase of CYP27B1 transcription in contrast to vehicle treated cells. Because a VDRE has not been identified thus far in the CYP27B1 promoter,

there is no evidence for a transcriptional regulation of CYP27B1 via the VDR pathway. Other mechanisms must explain the enhancement of CYP27B1 gene expression after calcitriol treatment. Regarding the existence of splice variants in glioblastoma multiforme, it is not possible to make conclusions about an increased CYP27B1 activity.

This study provides first evidence for different modes of action of calcitriol in glioblastoma multiforme. Depending on cell environment and possibly on different molecular profiles of the vitamin D_3 metabolism, there seem both proliferative and antiproliferative effects. The mechanisms behind these effects are likely to be rather complex: (i) Gene amplification or simply increased CYP27B1 expression, resulting not necessarily in a higher level of active enzyme but in a deregulation of transcription/translation of the enzyme. (ii) Deregulation of the tissue-specific expression of splice variants in glioblastoma multiforme, resulting in a higher level of inactive enzyme. (iii) A special catabolism of calcitriol in glioblastoma multiforme, resulting in a change of calcitriol levels or in the formation of additional vitamin D_3 metabolites with unknown effects. (iv) An elevated expression of CYP24 in contrast to normal brain that causes an increased degradation of calcitriol. (v) Low expression of VDR and the expression of another, not yet identified receptor, mediating proliferative effects.

Specifically, in the light of the large number of splice variants, any therapeutically concept should take into account the complexity of the vitamin D_3 metabolism in glioblastoma multiforme. The investigation of escape mechanisms in glioblastoma multiforme may result in new ways to manipulate glioblastoma multiforme growth employing effects of vitamin D_3 metabolites and therefore may lead to new modes of therapy.

References

1. Christakos S, Raval-Pandya M, Wernyi RP, Yang W. Genomic mechanisms involved in pleiotropic actions of 1,25-dihydroxyvitamin D_3. Biochem J 1996;316:361–71.
2. Nemere I, Szego CM. Early actions of parathyroid hormone and 1,25-dihydroxycholecalciferol on isolated epithelial cells from the rat intestine. Endocrinology 1981;109:2180–7.
3. Osborne JE, Hutchinson PE. Vitamin D and systemic cancer: is this relevant to malignant melanoma? Br J Dermatol 2002;147:197–213.
4. Zehnder D, Bland R, Williams MC, et al. Extrarenal expression of 25-hydroxyvitamin d(3)-1 α-hydroxylase. J Clin Endocrinol Metab 2001;86:888–94.
5. Neveu I, Naveilhan P, Menaa C, Wion D, Brachet P, Garabedian M. Synthesis of 1,25-dihydroxyvitamin D_3 by rat brain macrophages *in vitro*. J Neurosci Res 1994;38:214–20.
6. Jones G, Ramshaw H, Zhang A, et al. Expression and activity of vitamin D-metabolizing cytochrome *P*450s (CYP1α and CYP24) in human nonsmall cell lung carcinomas. Endocrinology 1999;140:3303–10.
7. Zehnder D, Bland R, Hughes SV, et al. Analysis of the tissue distribution of 1α-hydroxylase identifies novel extra-renal sites for the synthesis of 1,25-dihydroxyvitamin D_3. In: Norman AW, Boullion R, Thomasset M, editors. Vitamin D endocrine system. Riverside: University of California; 2000. p. 159–62.
8. Van Leeuwen JPTM, Pols HAP. Vitamin D: anticancer and differentiation. In: Feldman D, Glorieux FH, Pike JW, editors. Vitamin D. London: Academic Press; 1997. p. 1089–99.
9. Garcion E, Wion-Barbot N, Montero-Menei CN, Berger F, Wion D. New clues about vitamin D functions in the nervous system. Trends Endocrinol Metab 2002;13:100–5.
10. Trouillas P, Honnorat J, Bret P, Jouvet A, Gerard JP. Redifferentiation therapy in brain tumors: long-lasting complete regression of glioblastomas and an anaplastic astrocytoma under long term 1-α-hydroxycholecalciferol. J Neurooncol 2001;51:57–66.
11. Hansen CM, Binderup L, Hamberg KJ, Carlberg C. Vitamin D and cancer: effects of 1,25(OH)$2D_3$ and its analogs on growth control and tumorigenesis. Front Biosci 2001;6:820–48.
12. Maas RM, Reus K, Diesel B, et al. Amplification and expression of splice variants of the gene encoding the P450 cytochrome 25-hydroxyvitamin D(3) 1,α-hydroxylase (CYP27B1) in human malignant glioma. Clin Cancer Res 2001;7:868–75.
13. Ding S, Lake BG, Friedberg T, Wolf CR. Expression and alternative splicing of the cytochrome P-450 CYP2A7. Biochem J 1995;306:161–6.
14. Stimpfel M, Tong D, Fasching B, et al. Vascular endothelial growth factor splice variants and their prognostic value in breast and ovarian cancer. Clin Cancer Res 2002;8:2253–9.
15. Adams M, Jones JL, Walker RA, Pringle JH, Bell SC. Changes in tenascin-C isoform expression in invasive and preinvasive breast disease. Cancer Res 2002;62:3289–97.
16. Bartl F, Harris LC, Würl P, Taubert H. *MDM2* and its Splice variant messenger RNAs: expression in tumors and down-regulation using antisense oligonucleotides. Mol Cancer Res 2004;2:29–35.
17. Diesel B, Seifert M, Radermacher J, et al. Towards a complete picture of splice variants of the gene for 25-hydroxyvitamin D_3 1α-hydroxylase in brain and skin cancer. J Steroid Biochem Mol Biol 2004;89–90:527–32.
18. Munnia A, Schutz N, Romeike BF, et al. Expression, cellular distribution and protein binding of the glioma amplified sequence (GAS41), a highly conserved putative transcription factor. Oncogene 2001;20:4853–63.
19. Struss A-K, Romeike BFM, Munnia A, et al. PHF3-specific antibody responses in over 60% of patients with *glioblastoma multiforme*. Oncogene 2001;20:4107–14.
20. Lehmann B, Pietzsch J, Kampf A, Meurer M. Human ceratinocyte line HaCaT metabolizes 1α-hydroxyvitamin D_3 and vitamin D_3 to 1α,25-dihydroxyvitamin D_3 (calcitriol). J Dermatol Sci 1998;18:118–27.
21. Bland R, Walker EA, Hughes SV, Stewart PM, Hewison M. Constitutive expression of 25-hydroxyvitamin D_3-1α-hydroxylase in a transformed human proximal tubule cell line: evidence for direct regulation of vitamin D metabolism by calcium. Endocrinology 1999;140:2027–34.
22. Hsu JY, Feldman D, McNeal JE, Peel DM. Reduced 1α-hydroxylase activity in human prostate cancer cells correlates with decreased suspectibility to 25-hydroxyvitamin D_3-induced growth inhibition. Cancer Res 2001;61:2852–6.
23. Denner K, Vogel R, Schmalix W, Doehmer J, Bernhardt R. Cloning and stable expression of the human mitochondrial cytochrome *P*450 11B1 cDNA in V79 Chinese hamster cells and their application for testing of potential inhibitors. Pharmacogenetics 1995;5:89–96.
24. Seifert M, Rech M, Meineke V, Tilgen W, Reichrath J. Differential biological effects of 1,25-dihydroxyVitamin D_3 on melanoma cell lines *in vitro*. J Steroid Biochem Mol Biol 2004;89–90:375–9.
25. Jones G, Strugnell SA, DeLuca HF. Current understanding of the molecular actions of vitamin D. Physiol Rev 1998;78:1193–231.
26. Panda DK, Al Kawas S, Seldin MF, Hendy GN, Goltzman D. 25-hydroxyvitamin D 1α-hydroxylase: structure of the mouse gene, chromosomal assignment, and developmental expression. J Bone Miner Res 2001;16:46–56.
27. Hentze MW, Kulozik AE. A perfect message: RNA surveillance and nonsense mediated decay. Cell 1999;96:307–10.
28. Mitschele T, Diesel B, Friedrich M, et al. Analysis of the vitamin D system in basal cell carcinomas (BCCs). Lab Invest 2004;84:693–702.
29. Lokeshwar VB, Schroeder GL, Carey RI, Soloway MS, Iida N. Regulation of hyaluronidase activity by alternative mRNA splicing. J Biol Chem 2002;277:33654–63.
30. Jung V, Romeike BF, Henn W, et al. Evidence for focal microheterogeneity in *glioblastoma multiforme* by area-specific CGH on microdissected tumor cells. J Neuropathol Exp Neurol 1999;58:993–9.
31. Kamao M, Tatematsu S, Hatakeyama S, et al. C-3 epimerisation of vitamin D_3 metabolites and further metabolism of C-3 epimers: 25-hydroxyvitamin D_3 is metabolized to 3-epi-25-hydroxyvitamin D_3 and subsequently metabolized trough C-1α of C-24 hydroxylation. J Biol Chem 2004;279:15897–907.
32. Norman AW, Sergeev IN, Bishop JE, Okamura WH. Selective biological response by target organs (intestine, kidney, and bone) to 1,25-dihydroxyvitamin D_3 and two analogues. Cancer Res 1993;53:3935–42.
33. Bishof MG, Siu-Caldera ML, Weiskopf A, et al. Differentiation-related pathways of 1 α,25-dihydroxycholecalciferol metabolism in human colon adenocarcinoma-derived Caco-2 cells: production of 1α,25-dihydroxy-3epi-cholecalciferol. Exp Cell Res 1998;241:194–201.
34. Schuster I, Egger H, Astecker N, Herzig B, Schüssler M, Vorisek G. Selective inhibitors of CYP24: mechanistic tools to explore vitamin D metabolism in human keratinocytes. Steroids 2001;66:451–62.
35. Bouillon R, Okamura WH, Norman AW. Structure-function relationships in the vitamin D endocrine system. Endocr Rev 1995;16:200–57.
36. Reddy GS, Siu-Caldera ML, Schuster I, et al. Target tissue specific metabolism of 1α-25-dihydroxyvitamin D_3 through A-ring modification. In: Norman AW, Bouillon R, Thomasset M, editors. Vitamin D chemistry, biology and clinical applications of the steorid hormone. Riverside: University of California; 1997. p. 139–46.
37. Van den Bemd GJ, Pols HA, Birkenhager JC, Kleinekoort WM, van Leeuwen JP. Differential effects of 1,25-dihydroxyvitamin D_3-analogs on osteoblast-like cells and on *in vitro* bone resorption. J Steroid Biochem Mol Biol 1995;55:337–46.
38. Elias J, Marian B, Edling C, et al. Induction of

apoptosis by vitamin D metabolites and analogs in a glioma cell line. Recent Results Cancer Res 2003; 164:319–32.

39. Baudet C, Chevalier G, Chassevent A, et al. 1,25-Dihydroxyvitamin D_3 induces programmed cell death in a rat glioma cell line. J Neurosci Res 1996;46: 540–50.

40. Magrassi L, Butti G, Pezzotta S, Infuso L, Milanesi G. Effects of vitamin D and retinoic acid on human glioblastoma cell lines. Acta Neurochir (Wien) 1995; 133:184–90.

41. Naveilhan P, Berger F, Haddad K, et al. Induction of glioma cell death by 1,25$(OH)_2$ vitamin D_3: towards an endocrine therapy of brain tumors? J Neurosci Res 1994;37:271–7.

42. Zou J, Landy H, Feun L, et al. Correlation of a unique 220-kDa protein with vitamin D sensitivity in glioma cells. Biochem Pharmacol 2001;60:1361–5.

43. Schwartz GG, Whitlach LW, Chen TC, Lokeshwar BL, Holick MF. Human prostate cells synthesize 1,25-dihydroxyvitamin D_3 from 25-hydroxyvitamin D_3. Cancer Epidemiol Biomarkers Prev 1998;7: 391–5.

44. Lou YR, Laaksi I, Syvala H, et al. 25-Hydroxyvitamin D_3 is an active hormone in human primary prostatic stromal cells. FASEB J 2004;18:332–4.

45. Baran DT. Nongenomic actions of the steroid hormone 1 α,25-dihydroxyvitamin D_3. J Cell Biochem 1994;56:303–6.

46. Magrassi L, Adorni L, Montorfano G, et al. Vitamin D metabolites activate the spingomyelin pathway and induce death of *glioblastoma* cells. Acta Neurochir (Wien) 1998;140:707–13.

47. Zierold C, Mings JA, DeLuca HF. Regulation of 25-hydroxyvitamin D_3-24-hydroxylase mRNA by 1,25-dihydroxyvitamin D_3 and parathyroid hormone. J Cell Biochem 2003;88:234–7.

48. Monkawa T, Yoshida T, Hayashi M, Saruta T. Identification of 25-hydroxyvitamin D_3 1α-hydroxylase gene expression in macrophages. Kidney Int 2000;58: 559–86.

49. Hewison M, Freeman L, Hughes SV, et al. Differential regulation of vitamin D receptor and its ligand in human monocyte-derived dendritic cells. J Immunol 2003;170:5383–90.